J Electroceram (2010) 24:91–96
DOI 10.1007/s10832-008-9528-9

Polarization and piezoelectric properties of grain-oriented ferroelectric $Bi_5FeTi_3O_{15}$ ceramics prepared by magnetic-field-assisted electrophoretic deposition method

Muneyasu Suzuki · Yuji Noguchi · Tetsuo Uchikoshi · Masaru Miyayama

Received: 26 March 2008 / Accepted: 20 May 2008 / Published online: 19 June 2008

Abstract Magnetic-field-assisted electrophoretic deposition method has been employed for synthesizing *a*(*b*)-axis-oriented $Bi_5FeTi_3O_{15}$ ceramics, and the effects of grain orientation and microstructure on the polarization and piezoelectric properties have been investigated. Grain-oriented $Bi_5FeTi_3O_{15}$ ceramics with a high relative sintered density of 98% is shown to exhibit enhanced polarization and piezoelectric properties with a remanent polarization (P_r) of 19 μC/cm^2 and a piezoelectric strain constant (d_{33}) of 23 pm/V, which are much superior to those of randomly-oriented ceramics (P_r of 7 μC/cm^2 and d_{33} of 5 pm/V).

Keywords Bismuth layer-structured ferroelectrics · Magnetic field · Electrophoretic deposition · Piezoelectric

M. Suzuki (✉) · Y. Noguchi · M. Miyayama
Research Center for Advanced Science and Technology,
The University of Tokyo,
4-6-1 Komaba, Meguro-Ku,
Tokyo 153-8904, Japan
e-mail: muneyasu@crm.rcast.u-tokyo.ac.jp

Y. Noguchi
SORST, Japan Science and Technology Agency (JST),
4-1-8 Honcho, Kawaguchi-shi,
Saitama 332-0012, Japan

T. Uchikoshi
Fine Particle Processing Group, Nano Ceramics Center,
National Institute for Materials and Science,
1-2-1 Sengen, Tsukuba,
Ibaraki 305-0047, Japan

1 Introduction

Bismuth layer structured ferroelectrics (BLSFs) have attracted a great deal of attention from technological and scientific points of view. In the crystal structure of BLSFs, perovskite blocks composed of m (m=1, 2, 3, 4, 5) layers of BO_6 octahedra with A-site cations are sandwiched between Bi_2O_2 layers. It is recognized that the entire displacement of the perovskite blocks with respects to the Bi_2O_2 layers induces ferroelectric nature which appears mainly along the a-axis [1]. This Bi-layered structure leads to a high Curie temperature (T_C) [2, 3] and a large spontaneous polarization (P_s) along the a-axis [1, 4–6]. Additionally, along the c-axis BLSFs with even m number show paraelectricity whereas those with odd m number exhibit ferroelectricity [7, 8]. Hot forging [9–11] and templated grain growth method [12–15] have received considerable attention for preparation of grain-oriented (GO) ceramics of $Bi_4Ti_3O_{12}$ (BiT) and related ferroelectrics. These methods using the anisotropy of grain growth allow us to obtain GO-BLSF ceramics. Recently, colloidal processing taking advantage of high magnetic field [16–18] has been developed to obtain GO ceramics not only of alumina [16, 17, 19] and titania [20, 21] but also of BLSFs [18, 22–25]. In this processing, a magnetic field (B) of 10–12 T is applied to particles dispersed in a colloidal suspension. The interaction between the anisotropic magnetic susceptibility ($\Delta\chi$) of the particles and B leads to a magnetic torque (F) [19, 25], which is a driving force for the alignment of the particles along a specific crystallographic orientation in the colloidal suspension. Additionally, the colloidal processing leads to green compacts with homogeneous microstructure that is advantageous for obtaining high-density ceramics.

Here, we report the synthesis and properties of $Bi_5FeTi_3O_{15}$ (BFT) ceramics prepared by the *B*-assisted electrophoretic deposition (*B*-assisted EPD). BTF shows a high T_C of 787 °C [26] and is expected to have a large P_s along the *a*-axis. In the *B*-assisted EPD, we performed EPD under a high *B* in the colloidal suspension in which the particles are uniaxially aligned by *F*, leading to GO-green compacts. A degree of grain orientation is greatly enhanced by grain growth and densification of the compacts during sintering [16]. The *B*-assisted EPD [16] is an active method for synthesizing GO-green compacts in a short period of time of several tens minutes compared with the slip casting method.

Figure 1 shows the schematic representation of the *B*-assisted EPD developed for fabricating GO-ceramics of BLSFs. In this process, a high *B* of 10–12 T generated in a superconducting magnet is applied to the particles homogeneously dispersed in a stable colloidal suspension [Fig. 1(a)]. A magnetic torque (*F*) [18, 25] is exerted to the particles as a result of the interaction between $\Delta\chi$ and *B*. Even though $|\Delta\chi|$ is as small as 1×10^{-8} like BiT [17], the high value of *B* plays a critical role in *F*, because *F* is proportional to B^2 [25]. Since the use of a high *B* offers a sufficiently high *F* acting upon the particles, the particles are aligned along a specific orientation with respect to *B* to minimize the system energy [see Fig. 1(b)]. For the slip casting method [19], the solvent in the suspension is gradually eliminated under *B*, and then green compacts with oriented particles are obtained. For the *B*-assisted EPD, we performed EPD under a high *B* in the suspension in which the particles are uniaxially aligned by *F* [Fig. 1(c)], leading to GO-green compacts composed of BFT particles with the *a*(*b*) axis parallel to *B* [see Fig. 1(d)]. A degree of grain orientation is greatly enhanced by grain growth and densification of the compacts during sintering [16].

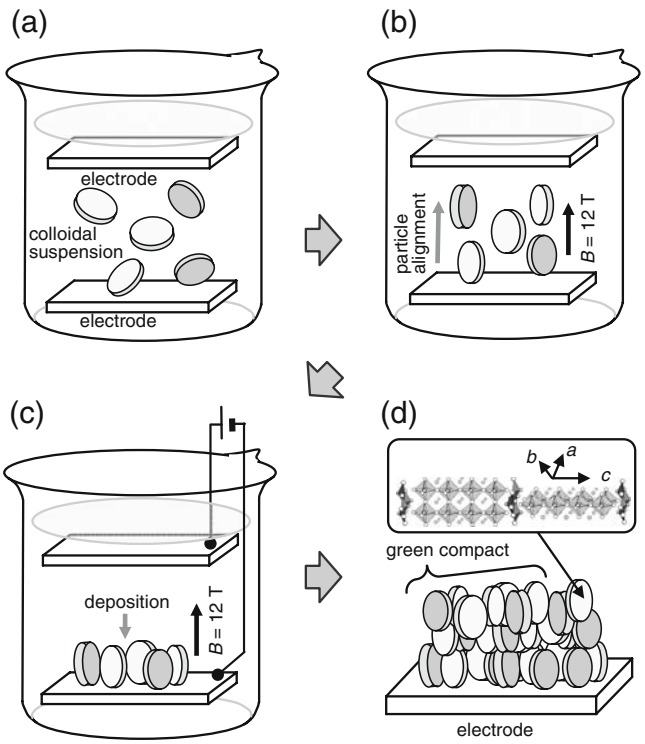

Fig. 1 Schematic representation of the *B*-assisted electrophoretic deposition (EPD) developed for fabricating grain-oriented (GO)-ceramics of BLSFs; (**a**) BFT particles are homogeneously dispersed in a stable colloidal suspension and (**b**) the particles are aligned along the *a*–*b* plane by applying *B*. (**c**) The particles are deposited by EPD under a high *B* of 12 T in the suspension, and (**d**) green compacts in which the particles are aligned along the *a*–*b* plane with respect to *B* are obtained

2 Experiment

BFT powder was synthesized by solid-state reaction. Stoichiometric mixtures of Bi_2O_3 (99.9999%), TiO_2 (99.99%) and Fe_2O_3 (99.99%) were thoroughly mixed and ground. The BTF particles which have an elongated or plate-like shape with a grain size of 1–4 μm were confirmed by scanning electron microscope (SEM) observations. In order to investigate a calcination temperature at which single-phase BFT is formed, the appropriate mixed powder was calcined at different temperatures from 800 to 1000 °C for 2 h in air. The optimized calcination temperature for synthesizing BFT powder was determined to be 900 °C. For obtaining green compacts by the *B*-assisted EPD, we dispersed the calcined powder homogeneously in ethanol with phosphoric ester and polyethylenimine using magnetic stirrer with the help of an ultrasonic horn. EPD was conducted for 60 min in a *B* of 12 T using a pair of facing Pd electrodes with an electrode spacing of 20 mm by applying an electric voltage of 200 V. In this processing, both electric and magnetic fields were applied along a vertical line, and the particles were deposited onto the bottom electrode. After the deposited bulk was drawn out from the suspension outside the magnet, the obtained green compact carefully dried for 1 week under no magnetic field. The completely dried green compacts were sintered at 1100 °C for 2 h in air. For comparison, randomly-oriented (RO) BFT ceramics were prepared by solid-state reaction using the same powder used for the EPD processing. The calcined powders were pressed into disks followed by cold isostatic pressing and then sintered at 1100 °C for 2 h in air.

Constituent phase, crystal structure, and grain orientation of the sintered ceramics were analyzed by x-ray diffraction (XRD). Microstructures were investigated by SEM. For the measurements of polarization and piezoelectric strain properties, the specimens were polished down to 0.2 mm

in thickness, and then Au dots of 1.0 mm in diameter were sputtered onto both surfaces. In GO-ceramics, electric field is parallel to the *B* direction of the ceramics.

3 Results and discussion

Figure 2 shows the XRD patterns measured on the surface of BFT ceramics together with the schematic 3D microstructures produced from the SEM images (Fig. 3). Both ceramics synthesized by the *B*-assisted EPD and solid-state reaction had a relative sintered density of 98%. Compared with RO-ceramics [Fig. 2(a)], the green compacts obtained by the *B*-assisted EPD [Fig. 2(b)] exhibited a slightly high intensity ratio of 200/020 to 119. This result clearly demonstrates that the alignment of the particles in the suspension induced by the *B* application remains even in the green compacts. Since the surface normal to the compacts and electrode is corresponding to the direction of *B*, the *a*(*b*)-axis orientation along *B* is established for BTF particles, which agrees well with GO-ceramics of BiT [22, 24] and $CaBi_4Ti_4O_{15}$ (*m*=4) [21] prepared by the slip casting under a high *B*. For GO-ceramics after the sintering, the peaks of 200/020 and 220 became marked as shown in Fig. 2(c). Densification followed by grain growth during sintering at 1100 °C of the green compacts promotes the *a*(*b*)-axis orientation. In addition, XRD pattern of BTF ceramics synthesized by EPD without *B* were almost the same as that of RO-ceramics. These results suggest that the grain orientation in BTF ceramics proceeds via two stages:

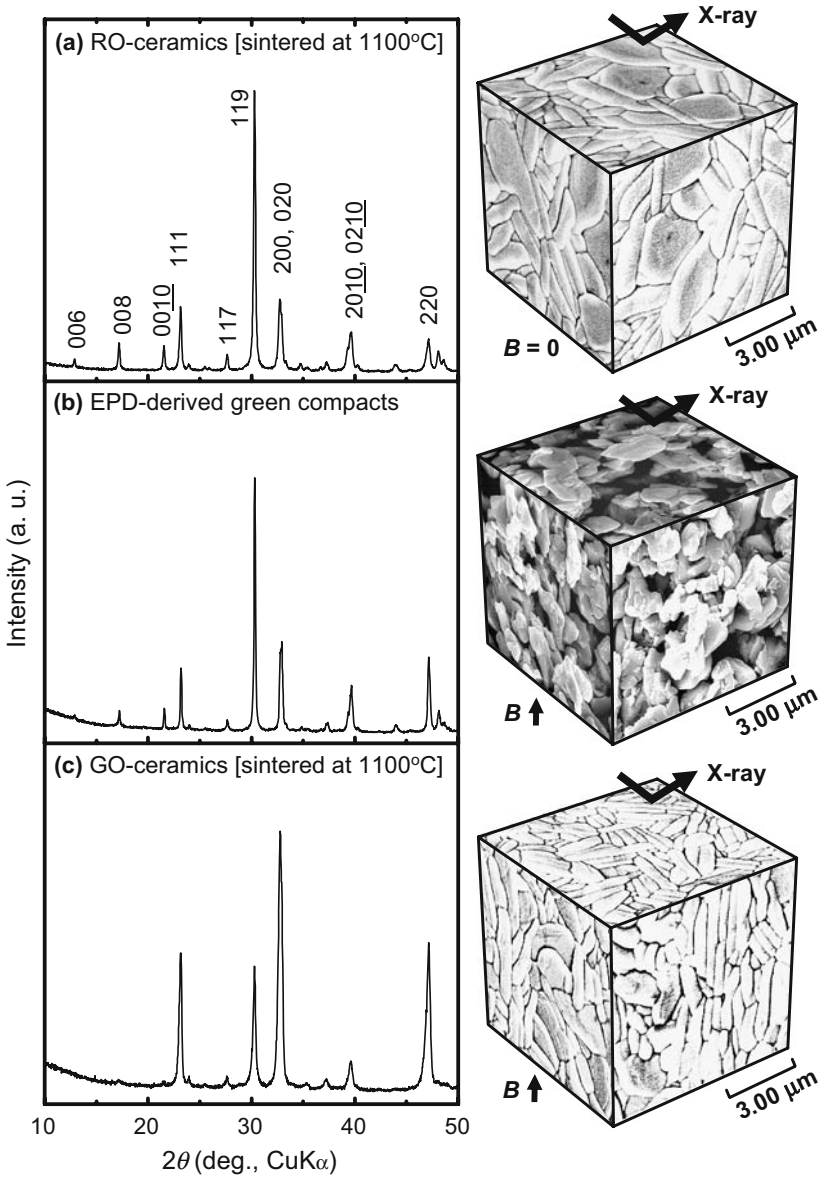

Fig. 2 XRD patterns of BTF ceramics measured on the surfaces of the bulk samples for (**a**) randomly-oriented (RO)-ceramics, (**b**) EPD-derived green compacts and (**c**) GO-ceramics together with the schematic 3D microstructures produced from the scanning electron microscope (SEM) images. The surface normal to the bulks is corresponding to the direction of *B*, as shown in (**b**) and Fig. 3(c)

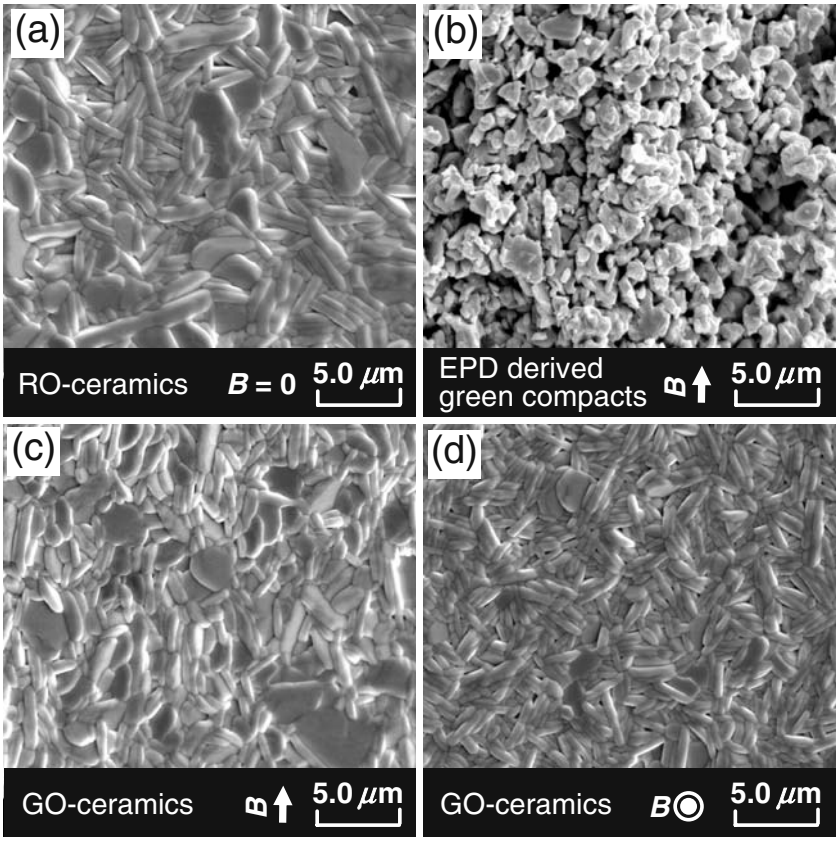

Fig. 3 SEM images of (**a**) RO-ceramics, (**b**) the cross-sectional surface of EPD-derived green compacts, (**c**) the cross-sectional surface of GO-ceramics and (**d**) the surface of GO-ceramics. The direction of *B* is depicted in arrows in (**b**) and (**c**) and *circles* in (**d**)

the first stage is the *a*(*b*)-axis alignment of the particles by *F* in the suspension [Fig. 2(b)] and this particle alignment is maintained in the green compacts obtained by EPD [Fig. 3(b)]; the second stage is the enhancement of the *a* (*b*)-axis orientation of the grains by densification followed by grain growth during the sintering process [Fig. 3(c)].

Here, we discuss the mechanism of particle alignment by the *B*-assisted EPD. We consider a colloidal suspension, in which magnetically anisotropic spherical particles with a volume of *V* are homogeneously dispersed by the repulsive force due to electrical double layer at the particle surface. In general, magnetic energy (*U*) of the particles in *B* is expressed as:

$$U = -\chi V B^2 / 2\mu_0, \tag{1}$$

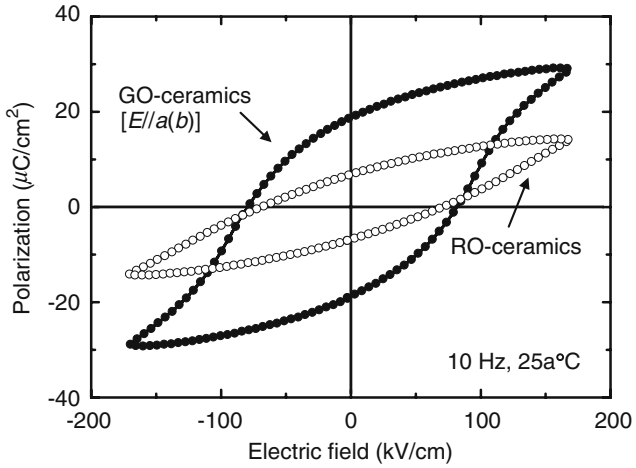

Fig. 4 Polarization hysteresis loops of RO- and GO-ceramics measured at 10 Hz (25 °C)

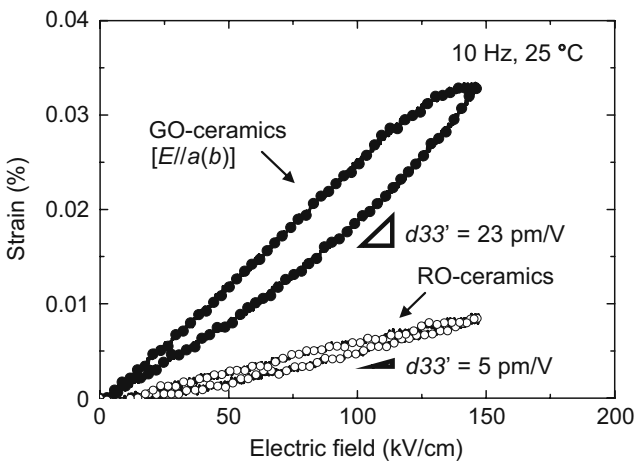

Fig. 5 Unipolar strain properties for RO- and GO-ceramics measured at 10 Hz (25 °C)

where μ_0 is the permeability of vacuum and χ is the magnetic susceptibility. For diamagnetic particles, U is lowered when B is parallel to the axis with a larger absolute value of χ ($|\Delta\chi|$). When a B applied to the particles is as high as 12 T, F acting upon the particles becomes significant not only for magnetic materials with a large $\Delta\chi$ but also for diamagnetic materials with an extremely low $|\Delta\chi|$ (and thus $|\Delta\chi|$), of about 1×10^{-8} [17]. Taking the angle (φ) between the axis with the largest $|\chi|$ (the $|\chi|_{max}$ axis) and B into account, we can express F as:

$$F = -\Delta\chi V B^2 \sin 2\varphi / 2\mu_0. \quad (2)$$

In the case of $F>k_BT$ (k_B and T are the Boltzmann constant and absolute temperature, respectively), the particles rotate until B // the $|\chi|_{max}$ axis is established. The large 200/020 XRD peak observed for GO-ceramics (Fig. 2(c)) indicates $|\chi_{a(b)}| < |\chi_c|$, i.e. $|\Delta\chi| = |\chi_c - \chi_{a(b)}|$ plays a dominant role for the particle alignment of BFT. The enhanced 220 peak in addition to 200/020, which is clearly seen in Fig. 2(c), indicates that the a–b plane of the BTF particles is aligned along B in the suspension, and that the difference between χ_a and χ_b is negligibly small.

Figure 4 represents the polarization properties of BTF ceramics measured at 10 Hz (25 °C) with a maximum electric field of 170 kV/cm. For GO-ceramics, electric field (E) was applied along the B direction, i.e., along the preferred a(b)-axis. GO-ceramics showed a remanent polarization (P_r) of 19 μC/cm^2, which was much larger than that of RO-ceramics (7 μC/cm^2). The values of coercive field (E_c) were almost the same for GO- (80 kV/cm) and RO-ceramics (70 kV/cm).

Figure 5 indicates the unipolar strain versus E at 10 Hz for the BFT ceramics (25 °C). A linear strain as a function of E was observed for both samples, indicating that non-180° domain rotation does not play a dominant role in these ceramics. The small hysteresis of the piezoelectric strain is preferable for practical applications such as high-precision actuators. The values of piezoelectric strain constant estimated from the slope of the strain properties (d_{33}) was 23 pm/V for the GO-ceramics, which was five times as large as that of the RO-ceramics (5 pm/V).

4 Conclusions

The B-assisted EPD has been employed for synthesizing a (b)-axis-oriented BFT ceramics, and the polarization and piezoelectric properties have been investigated. The grain orientation in BTF ceramics by the B-assisted EPD is suggested to proceed via two stages: the first stage is the a (b)-axis alignment of the particles in the suspension and this particle alignment is maintained in the green compacts; the second stage is the enhancement of the a(b)-axis orientation of the grains by densification followed by grain growth during the sintering process. Grain-oriented BFT ceramics showed a P_r of 19 μC/cm^2 and a d_{33} of 23 pm/V, which were much superior to those of randomly-oriented ceramics (P_r of 7 μC/cm^2 and d_{33} of 5 pm/V). It is demonstrated that the B-assisted EPD is effective for synthesizing grain-oriented BFT ceramics with superior polarization and piezoelectric properties.

Acknowledgement This study was partly supported by Industrial Technology Research Grant Program in 2006 from New Energy and Industrial Technology Development Organization (NEDO) of Japan.

Reference

1. S.E. Cummins, L.E. Cross, J. Appl. Phys. **39**, 2268 (1968) doi:10.1063/1.1656542
2. A.Z. Simoes, A. Ries, C.S. Riccardi, A.H.M. Gonzalez, E. Longo, J.A. Varela, J. Appl. Phys. **100**, 074110 (2006) doi:10.1063/1.2357419
3. H.X. Yan, H.T. Zhang, R. Ubic, M.J. Reece, J. Liu, Z.J. Shen, Z. Zhang, Adv. Mater. **17**, 1261 (2005) doi:10.1002/adma.200401860
4. Y. Noguchi, M. Miyayama, Appl. Phys. Lett. **78**, 1903 (2001) doi:10.1063/1.1357215
5. H. Irie, M. Miyayama, T. Kudo, Jpn. J. Appl. Phys. **40**, 239 (2001) doi:10.1143/JJAP.40.239
6. Y. Noguchi, M. Soga, M. Takahashi, M. Miyayama, Jpn. J. Appl. Phys. **44**, 6998 (2005) doi:10.1143/JJAP.44.6998
7. H. Irie, M. Miyayama, T. Kudo, J. Appl. Phys. **90**, 4089 (2001) doi:10.1063/1.1389476
8. K. Sakata, T. Takenaka, K. Shoji, Ferroelectrics **22**, 825 (1978)
9. T. Takenaka, K. Sakata, J. Appl. Phys. **55**, 1092 (1984) doi:10.1063/1.333198
10. T. Takenaka, K. Sakata, Ferroelectrics **38**, 769 (1981)
11. J.A. Horn, S.C. Zhang, U. Selvaraj, G.L. Messing, S. Trolier-McKinstry, J. Am. Ceram. Soc. **82**, 921 (1999)
12. T. Takeuchi, T. Tani, Y. Saito, Jpn. J. Appl. Phys. **39**, 5577 (2000) doi:10.1143/JJAP.39.5577
13. T. Tani, J. Ceram. Soc. Jpn. **114**, 363 (2006) doi:10.2109/jcersj.114.363
14. T. Kimura, T. Takahashi, T. Tani, Y. Saito, J. Am. Ceram. Soc. **87**, 1424 (2004)
15. T. Uchikoshi, T.S. Suzuki, H. Okuyama, Y. Sakka, J. Mater. Sci. **39**, 861 (2004) doi:10.1023/B:JMSC.0000012915.76707.ca
16. T.S. Suzuki, Y. Sakka, K. Kitazawa, Adv. Eng. Mater. **3**, 490 (2001) doi:10.1002/1527-2648(200107)3:7<490::AID-ADEM490>3.0.CO;2-O
17. Y. Doshida, K. Tsuzuku, H. Kishi, A. Makiya, S. Tanaka, K. Uematsu, T. Kimura, Jpn. J. Appl. Phys. **43**, 6645 (2004) doi:10.1143/JJAP.43.6645
18. Y. Sakka, T.S. Suzuki, J. Ceram. Soc. Jpn. **113**, 26 (2005) doi:10.2109/jcersj.113.26
19. T.S. Suzuki, Y. Sakka, Jpn. J. Appl. Phys. **41**, L1272 (2002) doi:10.1143/JJAP.41.L1272

20. Y. Sakka, T.S. Suzuki, N. Tanabe, S. Asai, K. Kitazawa, Jpn. J. Appl. Phys. **41**, L1416 (2002) doi:10.1143/JJAP.41.L1416
21. T.S. Suzuki, M. Kimura, K. Shiratsuyu, A. Ando, Y. Sakka, Y. Sakabe, Appl. Phys. Lett. **89**, 132902 (2006) doi:10.1063/1.2357868
22. A. Makiya, D. Kusano, S. Tanaka, N. Uchida, K. Uematsu, T. Kimura, K. Kitazawa, Y. Doshida, J. Ceram. Soc. Jpn **111**, 702 (2003) doi:10.2109/jcersj.111.702
23. K. Tabara, A. Makiya, S. Tanaka, K. Uematsu, Y. Doshida, J. Ceram. Soc. Jpn. **115**, 237 (2007) doi:10.2109/jcersj.115.237
24. W.W. Chen, Y. Hotta, T. Tamura, K. Miwa, K. Watari, Scr. Mater. **54**, 2063 (2006) doi:10.1016/j.scriptamat.2006.03.010
25. T. Sugiyama, M. Tahashi, K. Sassa, S. Asai, ISIJ Int. **43**, 855 (2003) doi:10.2355/isijinternational.43.855
26. G.N. Subbanna, T.N. Gururow, A.N.R. Rao, J. Solid State Chem. **86**, 206 (1990) doi:10.1016/0022-4596(90)90136-L